In-situ Multilayer Film Growth Characterization by Brewster Angle Reflectance Differential Spectroscopy

N. Dietz, D.J. Stephens, G. Lucovsky and K.J. Bachmann
North Carolina State University, Raleigh, NC 27695

ABSTRACT

Brewster Angle Reflectance Differential Spectroscopy (BARDS) has been proposed as an optical method for real-time characterization of the growth of thin films. BARDS is based on changes in the reflectivity, R_p, of parallel (p)-polarized light incident at, or near, the Brewster angle of the substrate material. Changes in R are sufficiently large to monitor layer growth, and to determine the thickness and the optical constants of the deposited film. In this paper we extend the method to multilayer film deposition. The derivative properties of R are correlated with differences in the optical constants of the two materials, and with the sharpness of their interface. We present spectra for $SiO_2/Si_3N_4/SiO_2/Si$, demonstrating some of these aspects of this new and effective approach to in-situ monitoring.

I. INTRODUCTION

During the last decade, with increasing use of thin film deposition techniques, the need for in-situ growth monitoring has resulted in the development of various characterization methods. Due to the nondestructive character and the real-time application, optical probe techniques such as reflectance-difference spectroscopy (RDS)[1,2], surface photo-absorption (SPA)[3], dynamic optical reflectivity (DOR)[4] and Brewster angle reflectance spectroscopy (BARS)[5] have been developed for in-situ characterization of the growth of thin films. For a transparent substrate a well defined Brewster angle exists where the reflection coefficient, r_p, of the component of the incident light polarized parallel to the plane of incidence, vanishes. For an absorbing substrate, the Brewster angle law has to be modified from the condition $R_p = 0$ to a reflectance minima condition $dR_p / d\varphi = 0$. This definition of the Brewster angle is then also called the pseudo-Brewster or first Brewster angle. It has been shown that the Brewster angle law can be generally formulated as a function of the complex optical functions $\varepsilon = \varepsilon_1 + i\,\varepsilon_2$, which apply to transparent as well as absorbing media[6].

Compared to transparent media, the influence of the absorbing media on the Brewster angle can be expressed as a shift in the angle φ_B at which $dR_p / d\varphi = 0$ and in an offset, i.e.

$R_p|_{\varphi_B} \geq 0$. The reflectivity $R_p|_{\varphi_B}$ lies in the order of 10^{-6} - 10^{-4} for weakly absorbing media and increases up to 10^{-2} for strong absorbing media, such as metals. Assuming the growth of a film with a certain optical dielectric function $\varepsilon = \varepsilon_1 + i\,\varepsilon_2$ on a substrate, the reflected light from the surface can be initially split in two contributions. First, a large contribution related to the bulk properties of the substrate and second, a small contribution due to the growing film. Setting the angle of incidence at the Brewster angle φ_B of the substrate, its bulk contribution is set to zero, which allows highly sensitive detection of the initial layer growth. Changes in the growth conditions, such as a variation in the growth rate, density fluctuations or changes in the optical function ε during the growth results in a change of the slope in the monitored reflectance spectrum or in a discontinuity in the derivative reflectance spectrum, respectively.

II. MODEL CONSIDERATION

In the modeling of the changes in the reflectance for multilayer film growth, homogeneous isotropic substrates and films are assumed. For monochromatic light which is parallel polarized to the plane of incidence, no perpendicular reflectance components, r_s, have to be considered as, only the parallel reflectance components, r_p, contribute to the reflectance amplitude. For brevity, the index p will be dropped in the following text.

Assuming an 'n' layer system; ambient / film 1 / ... / film n / substrate (see Fig. 1), the reflection coefficient from the (n-1)th to the nst layer, $r_{(n-1)n}$, , is given by:

$$r_{(n-1)n} = \frac{\varepsilon_{f_n} \sqrt{\varepsilon_{f(n-1)} - \varepsilon_a \sin^2\varphi_0} - \varepsilon_{f(n-1)} \sqrt{\varepsilon_{f_n} - \varepsilon_a \sin^2\varphi_0}}{\varepsilon_{f_n} \sqrt{\varepsilon_{f(n-1)} - \varepsilon_a \sin^2\varphi_0} + \varepsilon_{f(n-1)} \sqrt{\varepsilon_{f_n} - \varepsilon_a \sin^2\varphi_0}}, \tag{1a}$$

and reflection coefficient from the nth layer to the substrate, r_{ns}, is given by

$$r_{ns} = \frac{\varepsilon_s \sqrt{\varepsilon_{fn} - \varepsilon_a \sin^2\varphi_0} - \varepsilon_{f_n} \sqrt{\varepsilon_s - \varepsilon_a \sin^2\varphi_0}}{\varepsilon_s \sqrt{\varepsilon_{fn} - \varepsilon_a \sin^2\varphi_0} + \varepsilon_{f_n} \sqrt{\varepsilon_s - \varepsilon_a \sin^2\varphi_0}}. \tag{1b}$$

The phase factor Φ_n for the nth layer can be described by:

$$\Phi_n = \frac{2\,\pi\, d_{fn}}{\lambda} \sqrt{\varepsilon_{fn} - \varepsilon_a \sin^2\varphi_0}. \tag{2}$$

The thickness of the nth film is d_{fn}, φ_0 is the angle of incidence and ε_a and ε_s are the complex dielectric functions of the ambient and the substrate, respectively. The complex dielectric functions of the (n-1)th and nth films are indexed by ε_{fn-1} and ε_{fn}, respectively. Figure 1 shows

the reflected and transmitted waves for a 2 layer (ambient - film 1 - film 2 - substrate) system for a p-polarized light beam.

The reflectance amplitude rr_n can be calculated from a 'n' - 2x2 matrix multiplication

$$\begin{bmatrix} M_{11} & M_{12} \\ M_{21} & M_{22} \end{bmatrix} = \begin{bmatrix} 1 & r_{a1} \\ r_{a1} & 1 \end{bmatrix} \begin{bmatrix} 1 & r_{12} \\ r_{12}\, e^{-2j\Phi_1} & e^{-2j\Phi_1} \end{bmatrix} \begin{bmatrix} 1 & r_{23} \\ r_{23}\, e^{-2j\Phi_2} & e^{-2j\Phi_2} \end{bmatrix} \cdots\cdots \begin{bmatrix} 1 & r_{(n-1)n} \\ r_{(n-1)n}\, e^{-2j\Phi_n} & e^{-2j\Phi_n} \end{bmatrix}$$

$$\text{with } rr_n = \frac{M_{21}}{M_{11}} . \quad (3)$$

Figure 2 shows the calculated change in the reflectivity for a SiO_2-Si_3N_4-SiO_2 multilayer system grown on a Si substrate. The angle of incidence is chosen at 70 degrees. The chosen wavelength is 670 nm. The derivative spectrum of the reflectivity versus film thickness is also shown. This clearly reveals a discontinuity at the interface of each layer. The changes in the slope can be used to characterize the different dielectric functions for each film.

III. EXPERIMENT

The experimental arrangement is schematically shown in Fig. 3. A laser diode with λ=670nm and 6.5mW power is used as light source. The parallel light beam is split into a reference and a signal channel. The signal beam is polarized parallel to the plane of incidence, using a Glan-Thompson polarizer, P, with an extinction ratio smaller than 10^{-6}. The polarized light is focused onto the sample held at an angle of 70 degrees, which is close to the Brewster angle, φ_B, of the silicon substrate. The reflected intensity is detected by a photomultiplier tube, PMT, and processed using a preamplifier and lock-in amplifier technique. The laser intensity is monitored at the reference channel to correct light intensity fluctuations.

Thin films of SiO_2 and Si_3N_4 were deposited on a n-Si (100) substrate using remote plasma enhanced CVD processing described elsewhere[7]. The flow rates for SiO_2 deposition were 300 sccm He flow, 15 sccm oxygen flow and 7.5 to 25 sccm SiH_4/Ar (10% SiH_4 diluted in Argon) for growth rates of 50 Å/min to 200 Å/min, respectively. The flow rates for Si_3N_4 deposition were 300 sccm He flow, 25 sccm SiH_4/Ar flow and 10 to 20 sccm NH_3 flow introduced through a ring 5 cm above the substrate. Substrate temperature and process pressure were maintained at 300 °C and 300 mtorr, respectively. The plasma was created by RF excitation at 13.56 MHz with a RF power of 400 W.

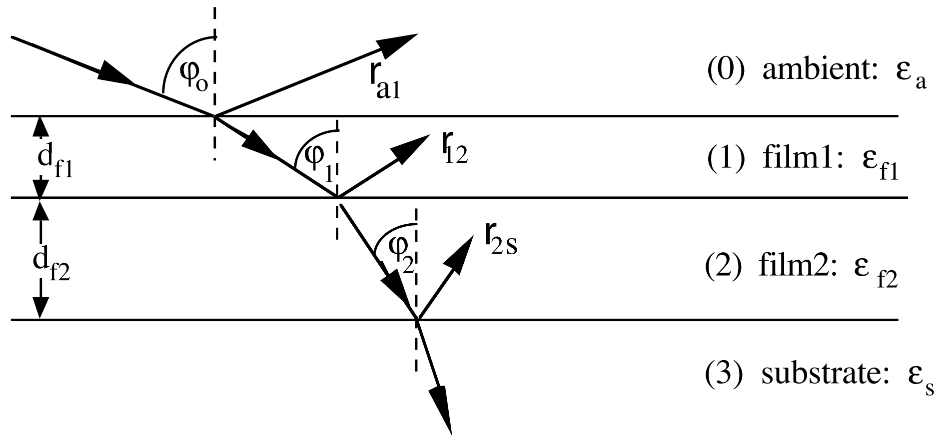

Fig. 1: Reflection of a plane wave (p-polarized to the plane of incidence) by a two layer-film structure between (0) ambient and (3) substrate. φ_0 is the angle of incidence; φ_1 and φ_2 are the angles of refraction; r_{a1}, r_{12} and r_{2s} are the reflection coefficients for the interfaces.

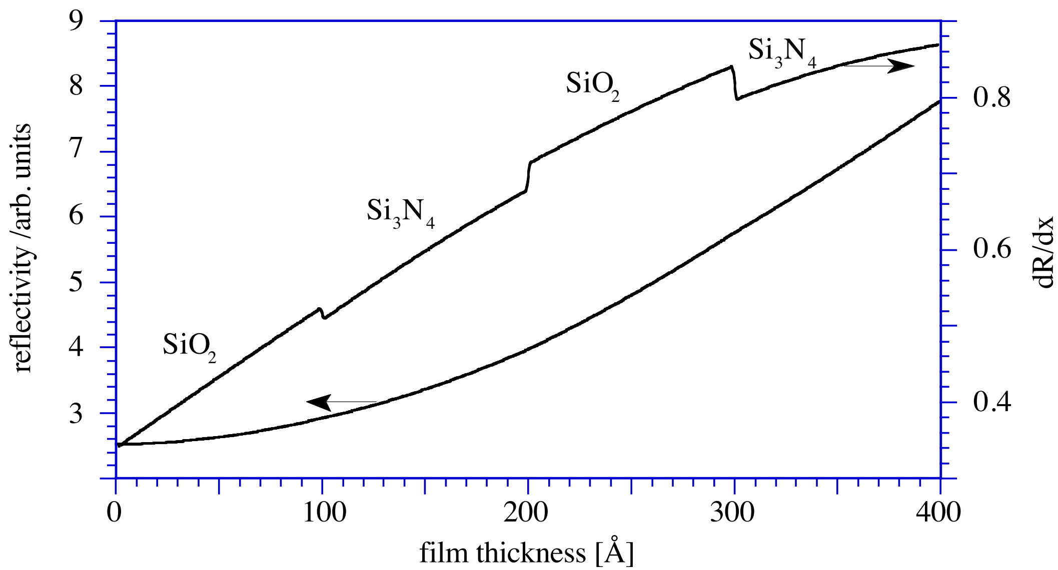

Fig. 2: Calculated changes in the reflectivity for SiO_2-Si_3N_4-SiO_2 multilayer deposition, on top of a Si substrate.

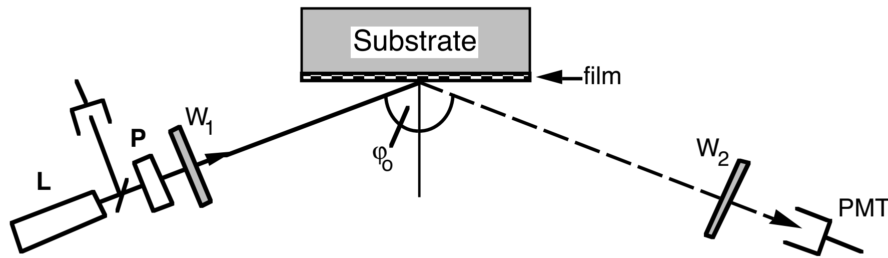

Fig. 3: Schematic diagram of the experimental setup; L: Laser; P: Glan Thompson polarizer; PMT: photo multiplier tube; W_1 and W_2 are the optical ports into the growth chamber.

IV. RESULTS AND DISCUSSION

The changes of the real-time monitored reflected intensity during the SiO_2 growth is shown in fig. 4 for two different processing conditions. The SiO_2 films are deposited at 300°C with a growth rate of ~100Å/min. Spectrum (b) in Fig. 4 shows the changes in the reflected intensity for SiO_2 growth starting with a hydrogen terminated Si (100) surface and Fig. 4 (a) shows the changes in the reflected intensity starting with a preoxidized Si surface. The preoxidation process involved a 60 sec He-oxygen plasma without SiH_4 flow at 300°C, which oxidized the Si surface, resulting in an uniform SiO_2 layer of about 6Å. The SiO_2 deposition parameters are identical for both spectra. The observed changes in the reflected intensity differ in the observed slope as well as the monitored intensity maxima .

To reveal the film thickness, the growth rate and the optical constants of the deposited SiO_2 layer, spectrum 4(a) is compared with a theoretical spectrum, calculated using eqs. (1) to (4) assuming one layer (SiO_2), ambient, $\varepsilon_a = 1$, and Si substrate, $\varepsilon_s = (15.20, 0.15)$. Figure 5 shows the experimental spectrum (as a function of thickness) compared with the theoretical spectrum for a SiO_2 layer. Best agreement is observed assuming a dielectric function of $\varepsilon_f = (2.14, 0.01)$ with a calculated growth rate of 85Å/min for the grown SiO_2 film, however, two discrepancies can be seen. First, the local minima of the experimental spectra are broadened and second, a large difference in the resolved peak maxima compared to the theoretical model can be observed. The broadened minima can be explained as a result of beam divergence, substrate surface roughness and depolarization effects in the optical ports of the growth chamber. The discrepancy in the intensity maxima is explained by the interaction of the laser beam with the RF-plasma, which is due to absorption of the laser light by excited hydrogen in the RF-plasma. This interaction results in a significantly lower detected intensity during the deposition process. Therefore, a calculation of the absolute reflectivity cannot be performed. Choosing a laser wavelength outside the absorption region eliminates this difficulty and permits the evaluation of possible additional sources of distortions of the experimental reflectance curve in future.

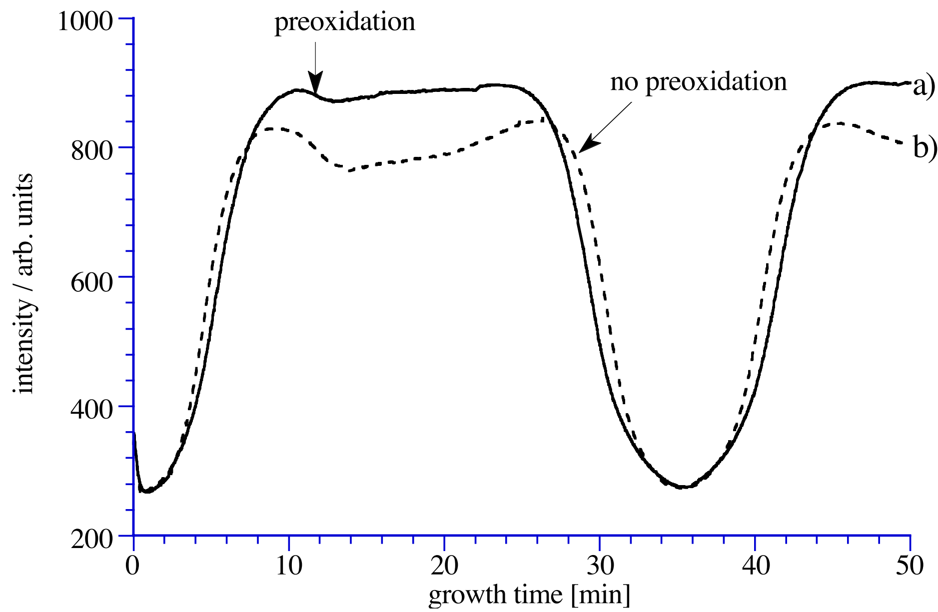

Fig. 4: Real-time monitoring of the reflected intensity during SiO_2 deposition, with and without preoxidation step.

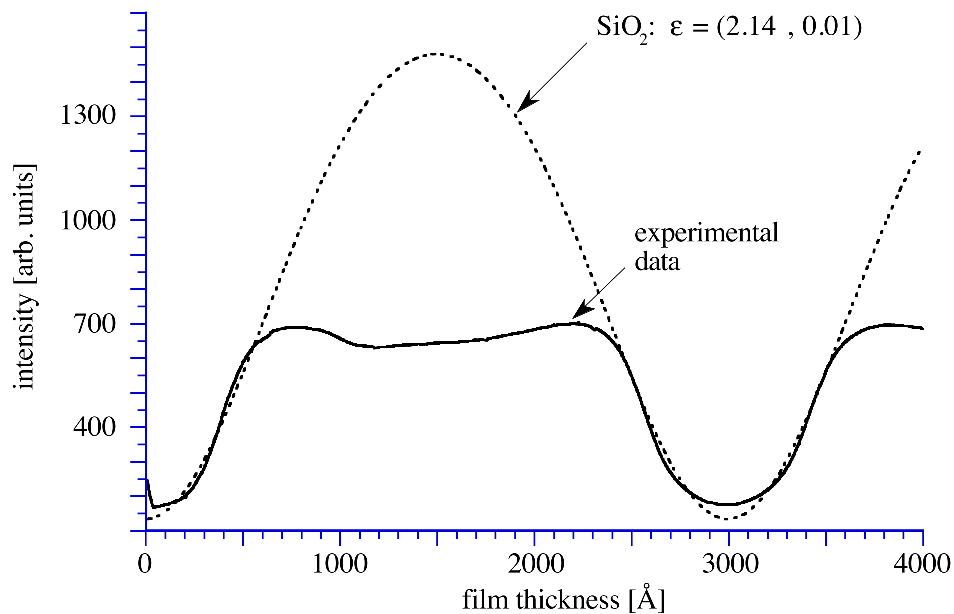

Fig. 5: Fitting of the experimental data (fulline) for the growth of SiO_2 on Si by a theoretical curve (dashed line) with a dielectric function (2.14, 0.01) at 670 nm.

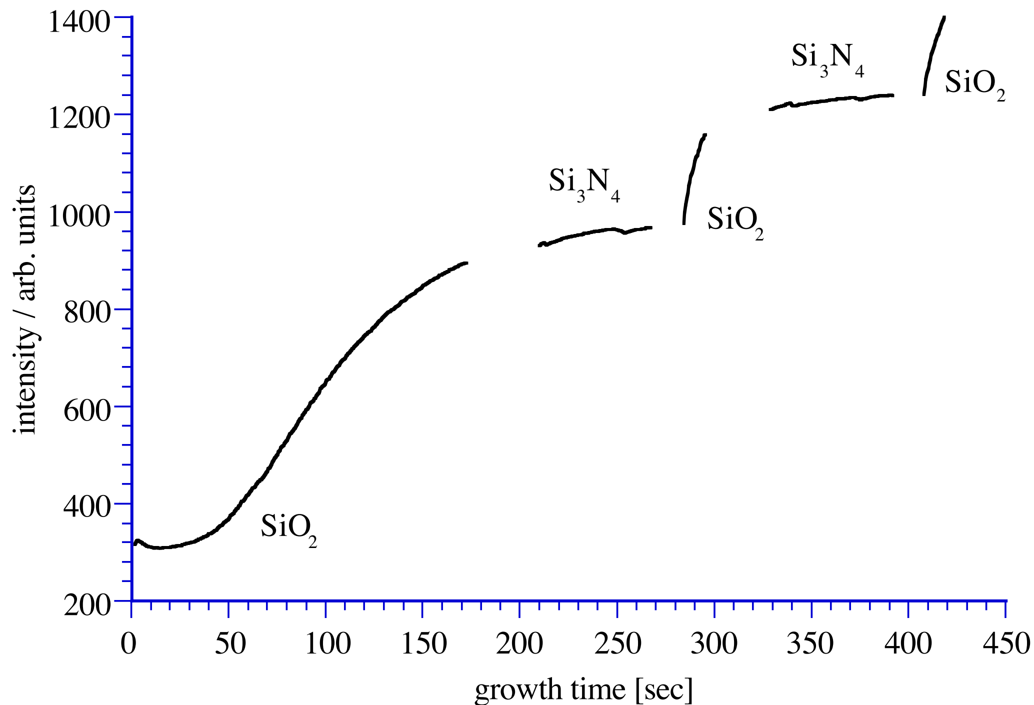

Fig. 6: Monitored changes in the reflected intensity during a SiO_2 - Si_3N_4 multilayer deposition.

Figure 6 shows the changes in the reflected intensity during a multilayer SiO_2 - Si_3N_4 growth starting with a H-terminated Si (100) surface. The SiO_2 was deposited with a growth rate of about 200 Å/min and the Si_3N_4 was deposited with a growth rate of about 55Å/min. Due to the interaction between the laser light and the applied plasma during the deposition process, a drop in the intensity occurred while switching the deposition from the SiO_2 process to the Si_3N_4 process. This resulted in a drop in the intensity of the reflected light. After 10 to 30 sec the process was stabilized. The observed changes in the slope of the reflected intensity versus time curve upon switching between SiO_2 and Si_3N_4 deposition are related to the differences in the growth rates and the dielectric functions of the deposited SiO_2 and Si_3N_4 films. If the growth rate for each deposition process is known, the intensity spectrum as a function of time can be converted into a film thickness scaling and the revealed changes in the slopes can be related to the optical constants for each film.

V. CONCLUSION

BARDS allows the real-time monitoring of multilayer film growth. Theoretical calculations show that differences in the dielectric functions for each film result in a discontinuity in the differential spectrum. First results for SiO_2 and Si_3N_4 film depositions show that the information obtained by BARS can be used to obtain the film thickness, the growth rate and optical constants of the deposited film. Results on multilayer SiO_2 - Si_3N_4 film deposition display changes in the slope of the monitored reflected intensity versus time curve upon switching between SiO_2 and Si_3N_4 deposition, which are related to the differences in the growth rates and optical constants of the deposited layers.

ACKNOWLEDGMENT

The authors would like to thank C.G. Parker for RPECVD processing. This research is supported by the NSF grant CDR 8721505.

REFERENCES

1 D.E. Aspnes, W.E. Quinn, M.C. Tamargo, M.A.A. Pudensi, S.A. Schwarz, M.J.S.P. Brasil, R.E. Nahory, and S. Gregory , Appl. Phys. Lett. **60**(10), 1244-6 (1992).

2 D.E. Aspnes, J.P. Harbison, A.A. Studna, and L.T. Florez ; Appl. Phys. Lett. **52**(12), 957-9 (1988).

3 N. Kobayashi, T. Makimoto, Y. Yamauchi, and Y. Horikoshi, J. Cryst. Growth **107**(1-4), 62-7 (1991).

4 J.V. Armstrong, T. Farrell, T.B. Joyce, P. Kightley, T.J. Bullough, and P.J. Goodhew, J. Crystal Growth **120**, 84-87 (1992).

5 N. Dietz and H.J. Lewerenz, Appl. Surf. Sci. **69**, 350-354 (1993).

6 H.J. Lewerenz, N. Dietz, J. Appl. Phys. **73** (10), 4975-87 (1993).

7 C.G. Parker, C. Silvestre, M. Watkins, R.T. Kuehn and J.R. Hauser, Proceedings of UGIM Symposium, May 1993.